Available online at www.sciencedirect.com

ScienceDirect

Procedia CIRP 55 (2016) 95 – 100

www.elsevier.com/locate/procedia

5th CIRP Global Web Conference Research and Innovation for Future Production

Optimization of WAAM deposition patterns for T-crossing features

Giuseppe Venturini[a]*, Filippo Montevecchi[a], Antonio Scippa[a], Gianni Campatelli[a]

[a]*Department of Industrial Engineering, University of Firenze, Via Santa Marta 3, 50139, Firenze, Italy*

* Corresponding author. Tel.: +39 0552758726. *E-mail address:* giuseppe.venturini@unifi.it

Abstract

Among emerging additive manufacturing technologies for metallic components, WAAM (Wire and Arc Additive Manufacturing) is one of the most promising. It is an arc based technology characterized by high productivity, high energy efficiency and low raw material cost. Anyway, it has some drawbacks limiting its diffusion in the industry. One is the open issue about the layer deposition strategy that must be manually optimized in order to reduce as possible the residual stress and strains, efficiently matching the geometrical characteristics of the component to build and assure a constant height for each layer. This work deals with the definition of deposition paths for WAAM. The choice of a path must be carried out as a compromise between productivity and material usage efficiency. In the present paper, the process to select an optimized strategy for the manufacturing of T-crossing features will be shown.

Peer-review under responsibility of the scientific committee of the 5th CIRP Global Web Conference Research and Innovation for Future Production

Keywords: Additive Manufacturing; Computer Aided Manufacturing (CAM); Welding

1. Introduction

Additive Manufacturing (AM) technologies have encountered disruptive development and diffusion in the recent years. Among such technologies there are some very promising in terms of cost savings both during the production and the life of the components [1]. In the industrial field, among the most interesting technologies there are the ones able to produce end-use metallic components. These can be classified in two macro-groups: 'Powder Based' (PB) and 'Wire Based' (WB) technologies. In the first group, the working principle consists in the selective melting of successive thin metallic powder layers spread by a recoater on a metal solid building plate. The powder can be melt using a laser beam (e.g. Direct Metal Laser Sintering, DMLS) or an electron beam (Electron Beam Melting, EBM), as can be seen in [2]. The part building has to be carried out in an inert atmosphere in the first case and in vacuum in the latter. Either the use of laser (or an electron beam) and a controlled building atmosphere denotes the necessity for a very expensive hardware. In the WB technologies, a wire is fed through a duct up to the deposition zone where the wire is melted using a laser beam, an electron beam or an electric arc. The first two cases require controlled atmospheres (similar to the ones for the PB technologies), while in the last case a shielding gas is spread all over the welding pool. The electric-arc-based technologies show very interesting advantages respect to all the other AM technologies for metallic components. These technologies have been named Wire and Arc Additive Manufacturing (WAAM) by Cranfield University that is among the most active research institutes on the development of such technologies [3]. WAAM technology has a lower accuracy respect to the powder based techniques (±0.2 mm against ±0.04 mm) [4], and cannot be used to produce very complex parts (such as molds with internal cooling). However, it is suitable for the production of very large parts (up to meters) with medium complexity (e.g. stiffened aeronautical panels). The use of WAAM technology can allow for a huge reduction in Buy to Fly Ratio (BTF) making this technology very attractive for the aerospace industry. The traditional approach for aerospace parts is to use machining operations, that implies the use of a rough from which the most of the material must be removed. Especially when using high cost material, this could lead to a

Peer-review under responsibility of the scientific committee of the 5th CIRP Global Web Conference Research and Innovation for Future Production
doi:10.1016/j.procir.2016.08.043

large economic impact on the overall production. This can be reduced thanks to the introduction of the WAAM process [3]. In this sense, some aerospace companies have established fruitful collaborations with the university of Cranfield [3, 5]. Since the surface finish of WAAM is not compatible with most of the functional surfaces, it is necessary to carry out a finishing operation. Relevant advantages of WAAM respect to PB process are the deposition rate and the cost. The deposition rate typically ranges from 1 kg/h to 4 kg/h for steel that is an order of magnitude higher than the one of PB techniques [3]. The hardware cost for WAAM is quite low if compared to the hardware for PB operations. In fact, it simply consists of a Cartesian (or robotic) device to position the welding torch, a power unit, a shielding gas source and a wire feeder unit [3, 6]. An environmental controlled build chamber may be required to weld just reactive materials like titanium [3]. Huge benefits can be achieved integrating WAAM and machining operations in a hybrid machine [7]. In fact, it would be possible to switch between additive and machining operations allowing for finishing zones of the component that will be inaccessible when the part is completed.

In order to increase the usability and diffusion of WAAM, it is important to provide tools and guidelines for the process planning phase, and in particular for the deposition toolpath definition [8]. The defined toolpath must match the geometrical characteristics and dimensions of the part taking into account the properties of WAAM. This work deals with the optimization of deposition toolpaths for WAAM in order to guarantee deposition-failure-free parts and maximize the deposition efficiency, that is defined as the ratio between the final part volume (after finishing operation) and the total deposited volume. In this sense, this work could help the diffusion of WAAM technology providing tools to remove some of the barriers still present in the process planning.

2. Deposition patterns for WAAM features: literature review and proposed approach

The generation of deposition patterns for WAAM has to take into account two important aspects: the resultant distortions/residual stresses of the final part and the deposition efficiency. In this context, deposition efficiency means both the avoidance of deposition failures (such as depressions) and the generation of the best toolpath able to manufacture a part which dimensions are as close as possible to the final desired geometry. This is achieved both setting the optimal welding parameters and generating a deposition toolpath that takes into account the geometry of the beads.

The basic thin-walled features that can be manufactured using a 3-axis WAAM Cartesian production station (like the one used for the presented activity) are cylinders, vertical walls, direct crossings and T crossings (Fig. 1).

In [9] the problems arising during the deposition of direct crossing and inclined walls have been investigated and several deposition strategies have been compared; the main evaluation parameter for direct crossings is the height of the deposited material in the central zone (where the two walls intersects): it has to be as close as possible to the average height of the walls far from the central zone in order to limit the amount of material to machine away in finish-machining operations, maximizing the deposition efficiency.

As depicted in [6] an important aspect to be solved is the compensation of the start and stop portions of the weld bead. In fact, an excess of material generally characterizes the starting zone, and a depression the end one.

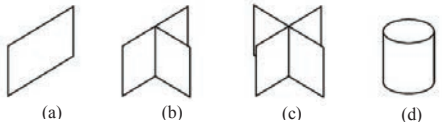

Fig. 1. 3-axis WAAM features; (a) vertical wall; (b) T crossing; (c) direct crossing; (d) cylinder, tubular.

Another fundamental tool for the process planning and toolpath generation for WAAM is a model or a database able to relate a specific welding set up with the resultant geometry of beads and walls. Several activities have been carried out on this topic for both traditional welding operations [10] and additive manufacturing operations [11]. In addition, several works [12,13] have been carried out to investigate optimization strategies for toolpath generation in order to mitigate residual stresses and distortions. Multi-directional slicing algorithms for layer additive manufacturing of metallic components has also been investigated [14].

The core of the present work is the individuation of deposition toolpaths that maximize deposition efficiency and reduce deposition time for thin-walled T-crossings that have not been already treated in literature. The parts and characteristics of T-crossings are listed in Fig. 2.

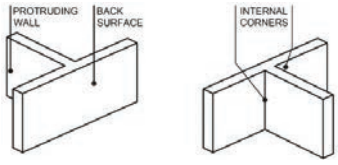

Fig. 2. Nomenclature of a T crossing feature.

In this work, WAAM deposition patterns for such feature are presented. It has been stated that WAAM parts have to be post-machined to match the required surface finish. Because of this, it is important to assess the machinability of WAAM manufactured material, and some efforts have already been carried out for example in [15]. However, it is also important to take into account the shape of the part to facilitate the machining operations. Regarding T-crossings, the most relevant issues for post machining could be the internal sharp corners, since these are not accessible using and end-mill. Creating toolpaths that reshape these zones adding fillets could improve the accessibility of the corners on the final part for machining and makes the toolpath more fluent (Fig. 3). The presence of fillets can also improve the mechanical properties, especially the fatigue-resistance. Besides, adding more material in the corners avoids the creation of voids and porosity. Of course, this excess material has to be machined away if a sharp corner is needed.

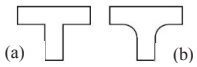

Fig. 3. Internal corners of T crossings; (a) sharp; (b) with fillet.

3. Deposition strategies for T crossings and evaluation parameters

3.1. Conformation and parameters of the proposed deposition strategies

Six different deposition strategies, shown in Fig. 4, for the T-crossing feature have been developed and compared. All the six strategies have been tested using the same welding parameters Keeping Fig. 4 as reference, it is possible to list the principles used to develop such deposition strategies. First of all, it is noticeable that all the strategies take into account the compensation of the different conformation of end and start portions of the weld beads: for every new weld bead the arc starts in the same point where has ended another one. This way, the effects brought by the difference between the start and the end portion are mitigated. Strategies S3, S3_I1 and S3_I2 feature fillets in the toolpath for the internal corners. The value of the radius of such fillets has been selected taking into account the width of the bead generated by the chosen welding parameters. The presence of the fillets is also useful to obtain a smooth and continuous toolpath with a limited number of start/stop phases and sharp corners. This will reduce spatter and problems due to axis slowdown.

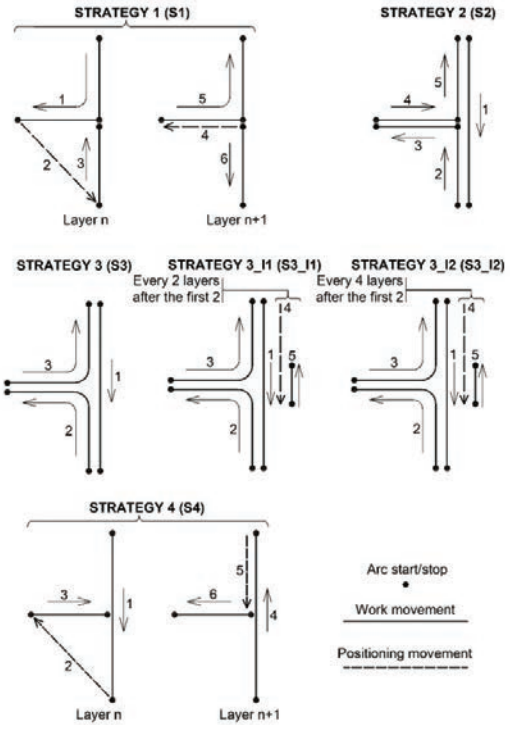

Fig. 4. Strategies S1 through S4.

For every strategy, 18 layers have been deposited and three parts have been built. Every 2 layers there is a pause of 70 seconds in order to allow for cooling of the part and measuring the height of the deposited material (see next sections for details).

3.2 Evaluation parameters to compare the deposition strategies

To compare and evaluate the different strategies, five evaluation parameters have been considered. The first one is the difference D (calculated every two layers) between the height of the central point and the average value of the heights of the points shown in Fig. 5 and named A1, A2, B1, B2, L1 and L2 that are far enough both from the central zone and from the wall ends [9]. This parameter, shown in Eq. 1, is directly related to the deposition efficiency: if the height in the C point is very close to the height of the other far points, less material will have to be removed.

$$D = C - \frac{A1 + A2 + B1 + B2 + L1 + L2}{6} \quad (1)$$

Another evaluation parameter is the presence or absence of fillets in the intersection.

To maximise the deposition efficiency, it is also important to achieve a back surface as flat as possible. The best result would be to obtain a planarity-error value of the back surface that is of the same order of magnitude of the waviness value brought by the layer-by-layer building procedure [16]. So, an error parameter to evaluate the difference between the real surface and the ideal one is considered (see further sections for details). The T-crossings built for the present work are hosted on a base plate with dimension 150x150 mm that enable them to be measured accurately on a Coordinate Measurement Machine (CMM). In general, WAAM is economically interesting for large parts, so it is important to limit the positioning movements between a pass and another: this has a positive effect on production time.

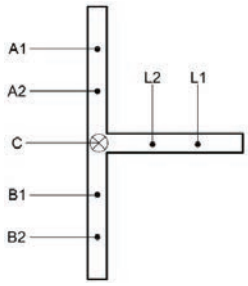

Fig. 5. Scheme for measurements of the height of deposited material.

To take into account also this aspect the ratio of Eq. 2 has been used. A deposition pattern will be as much time-effective (and so cost-effective) as much the ratio R is high.

$$R = \frac{active\ toolpath\ length}{total\ toolpath\ length} \quad (2)$$

Finally, since arc ignition and stop phases are often the cause of large amount of spatter, it is important to limit as much as possible the number of arc start/stop phases. So the number of start/stop phases will be taken into account as an evaluation parameter too.

4. The experimental set up

4.1. The test bench

The test bench used to manufacture the parts consists of a 3 axis CNC Cartesian machine and a MIG welder with integrated wire feeder. The CNC machine is a Roland Modela MDX-40 milling machine that has been retrofitted substituting the spindle with a bracket for the welding torch. The welder is analogic and is a Millermatic 300 by Miller. Through a PC-based numerical control it is possible to control the movements of the CNC Cartesian machine. Using a user-specified M code it is also possible to turn on and off the torch. The apparatus is provided with a device able to synchronize the ignition of the welding arc with the axis movement; this way the axis start moving only after the arc has ignited and the welding bead is deposited exactly from the programmed point without any delay.

Several combinations of welding parameters have been tested in order to define a set of welding parameters that generate a stable welding bead with reduced spatter. Besides, to limit the thermal input, all the parameters combinations are in the short circuit transfer mode range. Then, several walls have been built using the same strategy programmed for the T-crossings in order to measure the bead geometry and define accordingly the vertical increment in the NC code. Results of these preliminary tests are reported in Fig. 6, from which it is possible to calculate the value for the increment in the z direction that is equal to 1.5 mm. The width has also been acquired in order to be able to calculate the value of the radius for the fillets of the strategies S3, S3_I1, S3_I2. Of course, welding parameters strongly affect productivity. Every welding parameter set has to be a compromise between productivity and energy input achieving the desired wall width with the maximum allowed feed speed.

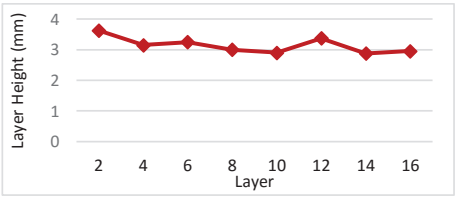

Fig. 6. Average Z increment every two layers.

4.2. Material, consumables and welding parameters

The material used to manufacture the parts is a 0.8 mm diameter wire of carbon steel (AWS ER70S-6). The shielding gas is STARGON C18, an industrial mix composed of 18% CO2 and 82% Argon. The parts have been manufactured on steel plates 150x150 mm, 12 mm thick made of S235JR steel. During the welding operations, the substrate rests on four pins protruding from the table of the machine and is fixed to the machine table using a bolted connection.

The welding parameters used to test the proposed deposition strategies are summarized in Table 1. The welding parameters have been kept constant for all the six strategies.

Table 1. The used welding parameters.

Parameter	Value
Base Current	50 A
Voltage	19 V
Wire Feed Speed	4.6 m/min
Welding Speed	300 mm/min
Nozzle to Work Distance	15 mm

4.3. Measurements acquired during and after the building process

Several measurements have been taken on the T-crossings during and after the building phase. For every strategy the data have then been averaged.

During the additive building process, measurements of the deposited material were taken every two layers during the 70 seconds pauses. The measurements are taken to monitor the relative growth between the central zone and the zone far from the intersection. The measurement points scheme is reported in Fig. 5. After the building was completed, the specimens were cleaned up with a steel brush and then the back surface was acquired with a coordinate measurement machine (Mitutoyo Euro-C A776). As shown in Fig. 7, the back surface has been acquired for a length of 65 mm in order to include the most critical zone that is the portion behind the protruding wall. Eight scanning lines have been performed spaced 2 mm one respect to the other. The acquired points in each line have a distance of 0.5 mm between them.

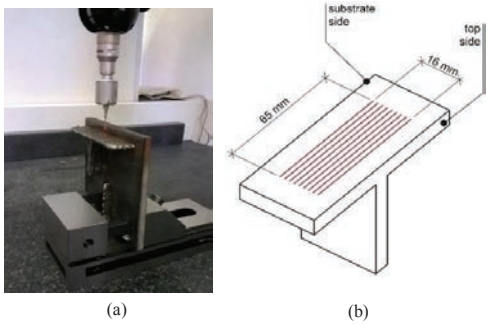

(a) (b)

Fig. 7. (a) Back surface acquisition on CMM machine; (b) Scanning scheme performed by the CMM machine.

5. Results and discussion

First, an overall visual analysis has been carried out, and then the six different strategies have been compared using the aforementioned evaluation parameters. From the visual analysis, it can be evinced that the S_3 strategy features the fillet as desired but also shows a dramatic deposition failure

(see Fig. 8) that inevitably causes an unacceptable drop in deposition efficiency and makes this strategy not suitable for building T-crossings. Hence, S3 is excluded from the following comparison.

Besides, the visual analysis confirms that the central zone of the back surface is the most critical one; in fact, in some strategies it shows a depression that reduces the deposition efficiency since it is necessary to machine away a high amount of material to obtain a flat surface. In other strategies, such depression is not so evident, that is of course a better case from an efficiency point of view.

Fig. 8. T-crossing built with S3 strategy; there is an evident deposition failure in the central zone (pointed by the red arrow).

In Fig. 9, the difference D between the height of the C point (Fig. 5) and the average heights of the other points is shown.

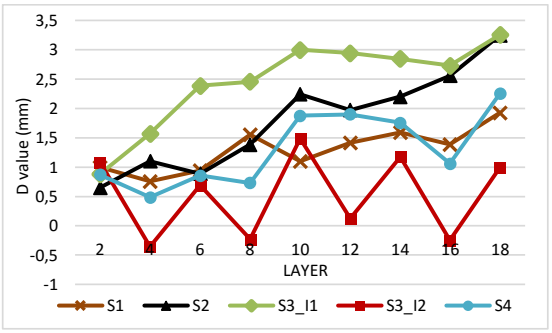

Fig. 9. The value of D for the six proposed strategies.

The bar plots shown respectively in Fig. 10 and Fig. 11 report the trends of the best-fit lines for the data of Fig. 9 and the average value of the parameter D across the 18 layers. It is noticeable that strategy S3_I2 achieves the best performance since the low slope of the best-fit line reveals that the height of the central point does not grow too much respect to the average height of the other zones during the building procedure. Besides, the average value of D is very small if compared to the other strategies and this means that the height in the central point is always very close to the one of other zones of the T crossing resulting in a high deposition efficiency. All this is important for the process stability: if the height of the C point would gradually increase too much respect to the average height of the far zones, the effective distance between the torch and the deposition plane would vary gradually leading to severe arc instability.

The data acquired with the CMM have been imported in Matlab® to plot the resultant 3D surface. For every different strategy, a best fit plane has been extracted from such surface considering the points far from the central zone (the one behind the protruding wall) that from the visual analysis seems to be the most critical one. Then, the differences between the heights of the scanned points of the central zone and the correspondent points of the best fit plane have been calculated. These have been divided in two vectors containing respectively the positive and the negative values. Of course the negative-value vector is the most relevant from a deposition efficiency point of view since it is related to the total amount of material that have to be machined away from the back surface. The norm of such vector is the parameter used to evaluate the quality of the back surface and is reported in Table 2 for all the six strategies.

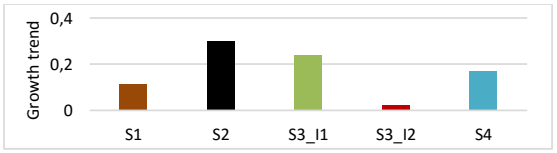

Fig. 10. Values of the slope of the best-fit lines for data shown in Fig. 9.

Fig. 11. Average values (across the 18 layers) of the D parameter for the proposed strategies.

In Fig. 12 the surface generated from the acquired points and the extracted best fit plane is shown for strategy S4 to visually explain the aforementioned concepts. In Table 2 there's a comparison between the six presented deposition strategies that takes into account all the considered evaluation parameters included the R value and the number of start/stop phases.

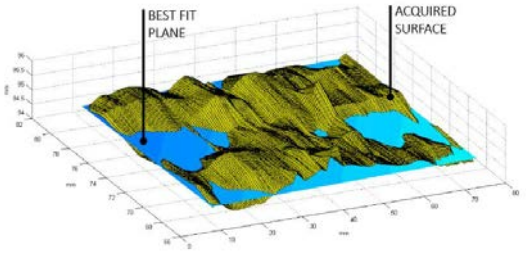

Fig. 12. Surface from acquired points (red) and best fit plane (cyan) for the strategy S4.

Looking at R and start/stop phases reported in Table 2 and excluding strategy S3 due to the deposition failure, it is possible to state that strategy S3_I2 achieves the best results in terms of start/stop phases with 32 start/stop phases. Besides, shows an acceptable R value.

Table 2. Comparison table for the six presented strategies.

Strategy	Failures	R	D	C Trend	Fillets	Start/ stop	Back surf. error	Evaluation
S1	No	0,64	1,3	0,11	No	54	1,60	Slow and non-continuous toolpath
S2	No	0,98	1,8	0,3	No	45	2,12	Fast toolpath but possible arc instability due to C point growth.
S3	Yes	0,99	-	-	Yes	27	-	Unacceptable for big deposition failure
S3_I1	No	0,75	2,45	0,24	Yes	36	0,74	Possible arc instability due to abnormal C point growth.
S3_I2	No	0,85	0,5	0,022	Yes	32	2,07	Good compromise between deposition efficiency, deposition time and process stability
S4	No	0,63	1,3	0,17	No	36	1,16	Acceptable deposition toolpath if sharp internal corners are needed

Concluding, strategy S3_I2 appears to be a good compromise between accessibility for post machining, deposition efficiency and deposition time. A T crossing built with S3_I2 strategy is reported in Fig. 13.

Fig. 13. A T crossing built using the S3_I2 strategy.

In effect, the performance for the back surface quality of S3_I2 is not excellent; anyway, its internal corners are accessible using an end mill and has a very continuous and fluent toolpath. In addition, the height of the C point (intersection zone) is very close to the average height value of the far zones resulting in a relevant arc stability and high deposition efficiency.

6. Conclusions

When building thin walled components through WAAM technology, the intersections between walls are among the most critical issues to face. As shown in this work, in the case of T-crossings, it is important to achieve a good quality of the back surface and to guarantee the arc stability assuring a regular growth of the central intersection zone. In this work a deposition pattern to optimally achieve these requirements has been individuated. The attention has also been focused on the quality of the internal corners that have to be accessible for the post machining operations and must not present voids and porosity in order to obtain a good surface quality and a robust part. In this sense, it has been determined that the introduction of a fillet in the internal corners results in a very fluent toolpath and, consequently, in a stable deposition process. If a sharp corner is needed, the excess of material brought by the fillet has to be totally machined away. Otherwise the presence of the fillet facilitates the finish machining of the part using an end-mill.

References

[1] Bikas H, Stavridis J, Stavropoulos P, Chryssolouris G. Design and Topology Optimization for Additively Manufactured Structural Parts: A Formula Student Case Study, (CAE), 6th BETA CAE International Conference, 10-12 May, Thessaloniki, Greece. Available Online 2015.
[2] Bikas H, Stavropoulos P, Chryssolouris G. Additive manufacturing methods and modelling approaches: a critical review, Int J of Adv Manuf Technol 2016; 83:389-405.
[3] Williams SW, Martina F, Addison AC, Ding J, Pardal G, Colegrove P. Wire + arc additive manufacuring. Mater Sci Tech Ser 2016.
[4] Ding D, Pan Z, Cuiuri D, Li H. Wire-feed additive manufacturing of metal components: technologies, developments and future interests. Int J Adv Manuf Technol 2015; 81:465-481.
[5] Sequeira Almeida P, Williams S. Innovative process model of Ti-6Al-4V additive layer manufacturing using cold metal transfer (CMT). Proceedings of the 21st Annual International Solid Freeform Fabrication Symposium, University of Texas Austin, TX, USA, 2010.
[6] Zhang Y, Chen Y, Li P, Male AT. Weld deposition-based rapid prototyping: a preliminary study. J Mater Process Tech 2003; 135:347-357.
[7] Karunakaran KP, Suryakumar S, Pushpa V, Akula S. Low cost integration of additive and subtractive process for hybrid layered manufacturing. Robot Cim-Int Manuf 2010; 26:490-499.
[8] Busachi A, Erkoyuncu J, Colegrove P, Martina F, Ding J. Designing a WAAM based manufacturing system for defence applications. Procedia CIRP 2015; 37:48-53.
[9] Mehnen J, Ding J, Lockett H, Kazanas P. Design study for wire and arc additive manufacture. Int. J. Product Development 19; 2014:2-19.
[10] Shoeb M, Parvez M, Kumari P. Effect of mig welding input process parameters on weld bead geometry on HSLA steel. International Journal of Enginnering Science and Technology 2013; 5:200-212.
[11] Ding D, Pan Z, Cuiuri D, Li H. A multi-bead overlapping model for robotic wire and arc additive manufacturing (WAAM). Robot Cim-Int Manuf 2015; 31:101-110.
[12] Mughal MP, Mufti RA, Fawad H. The mechanical effects of deposition patterns in welding-based layered manufacturing. Proceedings of the Institution of Mechanical Enginners, Part B: Journal of Engineering Manufacture 2007; 221:1499-1509.
[13] Mughal MP, Fawad H, Mufti RA, Siddique M. Deformation modelling in layered manufacturing of metallic parts using gas metal arc welding: effect of process parameters. Model Simul Mater Sc 2005; 13:1187-1294.
[14] Ding D, Pan Z, Cuiuri D, Li H, Larkin N, van Duin S. Automatic multi-direction slicing algorithms for wire based additive manufacturing. Robot Cim-Int Manuf 2016; 37:139-150.
[15] Montevecchi F, Grossi N, Takagi H, Scippa A, Sasahara H, Campatelli G. Cutting force analysis in additive manufactured AISI H13 alloy. Procedia CIRP 2016; 46:476-479.
[16] Martina F, Mehnen J, Williams SW, Colegrove P, Wang F. Investigation of the benefits of plasma deposition for the additive layer manufacture of Ti-6Al-4V. J Mater Process Tech 2012; 212:1377-1386.